JOURNAL OF Applied Polymer SCIENCE

Synthesis and Optical Properties of Cholesteric Liquid-Crystalline Oligomers Displaying Reversible Thermochromism

Ji-Wei Wang,[1] Bao-Yan Zhang[2]

[1]College of Pharmacy and Chemistry, Dali University, Dali 671000, People';s Republic of China

[2]Center for Molecular Science and Engineering, Northeastern University, Shenyang, 110004, People';s Republic of China

Correspondence to: J.-W. Wang (E-mail: jlwjw@sina.com)

ABSTRACT: A series of side-chain liquid crystalline oligomers (P_1–P_7) have been synthesized with cyclo(methylhydrogeno)siloxane and two cholesteric liquid crystalline monomers cholesteryl 4-(10-undecylen-1-yloxy)benzoate (M_1) and cholesterol 4-{6-[(4-(allyloxyl)-benzoyl]-hexanoxocarbonyl}-benzoate (M_2). The chemical structures and liquid crystalline properties of the synthesized oligomers were investigated using various experimental techniques such as FTIR, ^{1}H-NMR, DSC, POM, and XRD. All monomers and chiral oligomers show a cholesteric mesophase with very wide mesophase temperature ranges. They appear highly thermally stable with decomposition temperatures (T_d) at 5% weight loss greater than 300°C. The optical properties of the oligmers have been characterized by reflection spectra and optical rotation analysis. All synthesized oligomers display colors at room temperature, and show reversible thermochromism within a wide temperature range (>120°C). The λ_{max} values of the oligomers also nearly coincide during the first, second, and third heating cycles. The specific rotation of each oligomer is very sensitive to temperature, and the specific rotation value of P_3 smoothly changes from $-21.7°$ to $-0.7°$ when it is heated. The optical properties of the oligomers offer tremendous potential for various optical applications. © 2013 Wiley Periodicals, Inc. J. Appl. Polym. Sci. 000: 000–000, 2013

KEYWORDS: liquid crystals; phase behavior; optical properties

Received 7 December 2012; accepted 27 March 2013; Published online

DOI: 10.1002/app.39320

INTRODUCTION

Chiral materials have been extensively studied due to their unique properties originating from their atomic chiral centers and helical conformations. As a unique material, helical polymers have attracted great attention for their chiral structure and the resulting chiro-optical properties.[1–5] In synthetic chiral polymers, molecular helicity control can be achieved not only by varying the molecular chirality, but also via repeating units, hydrogen bonding, side chains, and block copolymers. When molecular chirality is introduced into liquid-crystalline polymers (LCPs), chiral LC phases with helical morphology are induced, resulting in a series of potential applications in optics and electro-optics.[6–8] On the other hand, side-chain LCPs combine optical and electro-optical properties of low molecular weight liquid crystals with mechanical properties and easy processing of liquid crystal polymers.[9–14] Chiral LCPs may exhibit a marvelous variety of liquid crystalline phases, including the chiral smectic C^* phase, the cholesteric phase, and the blue phases.[15–17]

Recently, chiral side-chain LCPs and oligomers composed of chiral mesogens have gained both industrial and scientific interests because their additional properties such as piezoelectricity, ferroelectricity, and pyroelectricity are associated with the symmetry breaking induced by molecular chirality.[18–23] Furthermore, the basic research on optical properties and its application have grown substantially. Cholesteric liquid crystals are chiral nematics which show a periodic helical structure, where the handedness of the constituent molecules leads to the orientation of the local nematic director to vary in space. The director is perpendicular to the helix axis, and its orientation varies linearly along this axis in the helical cholesteric structure axis. The periodic helical structure of cholesteric liquid crystals results in a selective reflection band. In this band, circularly polarized light with the same handedness as the cholesteric liquid crystals is reflected totally. The edges of the reflection band are at the free space wavelengths that are equal to the reflective indices multiplied by the pitch. In the helical cholesteric structure, the spatial period of the structure is the pitch. Cholesteric LCPs with the unique property of selective reflection

Additional Supporting Information may be found in the online version of this article.

of circularly polarized light have presented great potential for various optical applications.[24–31] However, the detailed relationship between the structure and optical properties of LCPs remains unclear so far.

To achieve a better understanding of the influence of molecular structures on the helical twist sense and the optical properties, we have synthesized a series of cyclosiloxane-based cholesteric LC oligomers by use of two different cholesteric monomers cholesteryl 4-(undec-10-en-1-yloxy)benzoate (M_1) and cholesteryl 4-{6-[(4-(allyloxyl)-benzoyl]-hexanoxocarbonyl}-benzoate (M_2). The generic structure of the oligomers is shown in Figure 1.

EXPERIMENTAL

Material and Measurements

Terephthaloyl dichloride, *p*-hydroxybenzoic acid, cholesterol, bromopropene, hexane-1,6-diol, *N*, *N*′-dicyclohexylcarbodiimide (DCC), dimethylaminopyridine (DMAP), hexachloroplatinic acid hydrate, and Cyclo(methylhydrogeno)siloxane (CMHS; M_n=200–300) were obtained from Jilin Chemical Industry Company and used without any further purification. Pyridine, sulfuric acid, thionyl chloride, toluene, ethanol, chloroform, tetrahydrofuran (THF), and methanol were purchased from Shenyang Chemical. Pyridine was purified by distillation over KOH and NaH before using.

^{1}H-NMR (300MHz) spectra were obtained with a Varian Gemini 300 NMR Spectrometer (Varian Associates, Palo Alto, CA) with Fourier transform using dimethyl sulfoxide-d_6 (DMSO-d_6) or $CDCl_3$ as a solvent and tetramethylsilane (TMS) as an internal standard. FTIR spectra of the synthesized polymers and monomers in solid state were obtained by the KBr method performed on PerkinElmer instruments Spectrum One Spectrometer (PerkinElmer, Foster City, CA). Thermal transition properties were characterized by a NETZSCH instrument DSC 204 (Netzsch, Wittelsbacherstr, Germany) at a heating rate of 10°°C min^{-1} under a nitrogen atmosphere. Phase transition temperatures were collected during the second heating and the first cooling scans. Visual observation of liquid crystalline transitions and optical textures under cross polarized light was performed by a Leica DMRX (Leica, Wetzlar, Germany) POM equipped with a Linkam THMSE-600 (Linkam, Surrey, UK) hot stage. X-ray diffraction (XRD) of the samples were performed using Cu $K\alpha$(λ = 1.54056 Å) radiation monochromatized with a Rigaku DMAX-3A X-ray diffractometer. Reflection spectra were measured by PerkinElmer instruments Lambda 950. Measurements of optical rotation (α) were carried out with a PerkinElmer instrument Model 341 Polarimeter using the D line of a sodium vapor lamp.

Synthesis of Liquid-Crystalline Monomers

Synthesis of Cholesteryl 4-(10-undecylen-1-yloxy)benzoate (M_1). 4-(10-Undecylen-1-yloxy)benzoate (M_1) was prepared according to previous reports.[32] Yield: 72%. m.p.: 68.6°C. IR (KBr, cm^{-1}): 3076 (—CH), 2961, 2859(CH_3, CH_2), 1733 (C═O), 1645 (C═C), 1605, 1510 (Ar). ^{1}H-NMR ($CDCl_3$, δ): 0.62–2.64 [*m*, 59*H*, —$(CH_2)_8$—, and CH_3—, —CH_2— and —CH— in cholesteryl); 4.91–5.04 (*m*, 2*H*, CH_2═CH—); 4.83–4.85 (*m*, 1*H*, cholesteryl —CH— in ester linkage); 5.41 (*m*, 1*H*, ═CH— in cholesteryl); 5.83 (*m*, 1*H*, CH_2═CH—); 7.16–8.08 (*m*, 4*H*, Ar-H).

Synthesis of Cholesteryl 4-{6-[(4-(allyloxyl)-benzoyl]-hexanoxocarbonyl}-benzoate (M_2). 4-Allyloxy-benzoic acid was synthesized according to a reported procedure.[33] 4-Allyloxy-benzoic acid (20.0 g, 0.112 mol), hexane-1,6-diol (47.2 g, 0.4 mol) and 2.0 mL of sulfuric acid were added into a round flask. The mixture was stirred at room temperature for 3 h, then heated to 80°C and kept for 14 h to ensure that the reaction finished. The excess hexane-1,6-diol was distilled under reduced pressure, and 24.0 g of 6-hydroxyhexyl 4-(allyloxy) benzoate.

Cholesterol (38.7 g, 0.10 mol) and 16 mL pyridine were dissolved in 50 mL dry chloroform. It was added dropwise with 450 mL chloroform solution of terephthaloyl dichloride (121.2 g, 0.60 mol) at room temperature. The reaction mixture was stirred at room temperature for 1 h, then heated to 60°C and kept for 18 h in a water bath to ensure that the reaction finished. Then all chloroform was distilled out. The precipitates were isolated by filtration and dried in a vacuum oven. Recrystallization in alcohol results in white crystals of intermediate cholesteryl 4-carboxyl-benzoate. Yield: 75%. m.p.: 161.6°C.

The intermediate cholesteryl 4-carboxyl-benzoate (77.4 g, 0.20 mol), DCC (41.2 g, 0.20 mol), and DMAP (6.1 g, 0.05 mol) were dissolved in 200 mL dry THF. It was added dropwise with

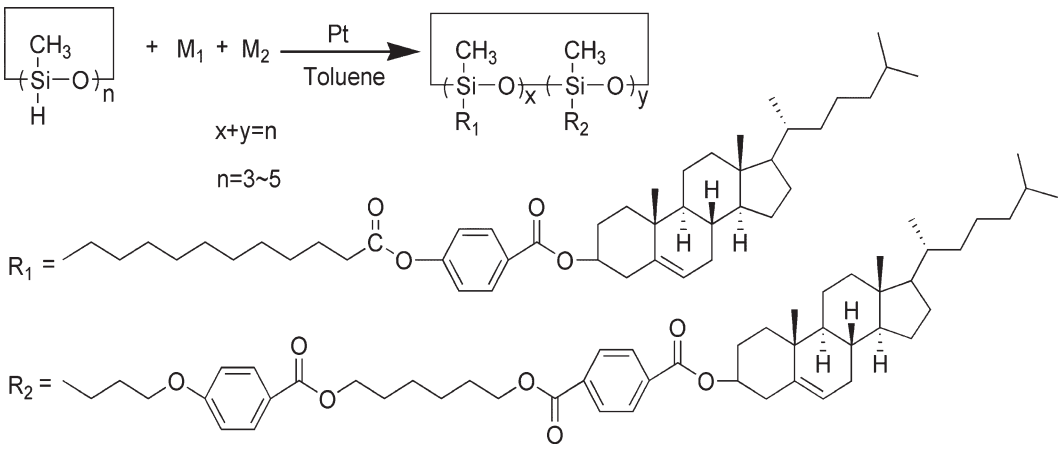

Figure 1. The generic structure of the oligomers.

Table I. Polymerization, Specific Rotation and the Max Selective Reflection Wavenumbers of the Oligomers

	Feed (mmol)		M_2/M_1[a]		λ_{max}[c]
Sample	M_1	M_2	%	$[\alpha]_D$[b]	(nm)
P1	4.0	0.0	0.00	−23.6	548
P2	3.6	0.4	13.1	−22.9	537
P3	2.8	1.2	43.6	−21.7	533
P4	2.0	2.0	51.2	−20.8	519
P5	1.2	2.8	2.43	−20.1	508
P6	0.4	3.6	91.8	−19.2	499
P7	0.0	4.0	100.0	−18.3	491

[a] Final molar ratio, estimated by ^{1}H-NMR spectroscopy.

[b] Specific rotation of oligomers, 0.1 g in 10 mL $CHCl_3$.

[c] The max selective reflection wavelengths of the oligomers at 25°C.

THF solution of 6-hydroxyhexyl 4-(allyloxy) benzoate (49 g, 0.20 mol) at room temperature. The reaction mixture was stirred at room temperature for 48 h to ensure that the reaction finished. Then the mixture was filtered, and the filtration liquor was distilled under reduced pressure. The residue was recrystallized by alcohol to obtain 25.6 g of liquid crystalline monomer cholesteryl 4-{6-[(4-(allyloxyl)-benzoyl]-hexanoxocarbonyl}-benzoate. Yield: 65%. $[\alpha]_D^{20} = -29.8°$, $c = 1$, chloroform, m.p.: 127.0°C. IR (KBr, cm^{-1}): 2927, 2854 (—CH_2—, CH_2= and =CH), 1726, 1717, (C=O), 1604, 1507 (Ar), 1275 (C—O—C). ^{1}H-NMR ($CDCl_3$, δ): 0.92–2.14 (*m*, 51*H*, CH_3—, —CH_2—, and —CH— in cholesteryl groups and in —$COOCH_2CH_2CH_2CH_2CH_2CH_2OOC$—); 4.36–4.87 (*m*, 7*H*, =$CHCH_2O$—, —$COOCH_2$—, and cholesteryl —CH— in ester linkage); 5.32–5.65 (*m*, 3*H*, CH_2=CH— and =CH— in cholesteryl groups); 6.03–6.10 (*m*, 1*H*, CH_2=CH—); 6.94–8.10 (*m*, 8*H*, Ar-H).

Synthesis of the Oligomers

For the synthesis of oligomers P_1–P_7, the same method is adopted. The polymerization and specific rotation are summarized in Table I. The synthesis of oligomer P_3 is given as an example. Chiral liquid-crystalline monomers M_1 (2.8 mmol), M_2 (1.2 mmol), and CMHS (1.0 mmol) were dissolved in 50 mL of dry, fresh distilled toluene. To the stirred solution, 2 mL of H_2PtCl_6/THF (0.50 g hexachloroplatinic acid hydrate dissolved in 100 mL THF) were added and heated under nitrogen and anhydrous conditions at 65°C for 24 h. Then the mixture was cooled and poured into methanol. After filtration, the product was dried to obtain polymer in the yield of 92%. IR (KBr, cm^{-1}): 2958, 2868 (CH_3— and —CH_2—), 1716–1715 (C=O), 1610, 1507 (Ar), 1261, 1120–1078 (Si—O—Si). ^{1}H-NMR ($CDCl_3$,δ): 0.48–0.50 (*m*, Si—CH_2), 1.28–2.68 (*m*, —CH_2—), 4.82–4.86 (*m*, cholesteryl —CH— in ester linkage), 4.40–4.61 (*m*, —OCH_2—), 5.30–5.44 (*m*, =CH— in cholesteryl groups), 6.95∼8.10 (*m*, Ar–H).

RESULTS AND DISCUSSION

Syntheses

The structures of M_1 and M_2 are characterized by IR and ^{1}H-NMR spectra, which is consistent with the predication, and reveals the high chemical purity of these monomers.

The structures of the synthesized oligomers were obtained by IR spectra. Oligomer P_3 contains the representative features for all polymers. The disappearance of the CMHS Si—H stretching at 2160 cm^{-1} and the olefinic C=C stretching band at 1635 cm^{-1} indicates successful incorporation of monomers into the polysiloxane chains. The ^{1}H-NMR spectra of P_3 and its chemical structure are shown in supporting information. No signal characteristic of terminal olefinic moiety and Si—H is observed in the ^{1}H-NMR spectra, i.e., the Si—H at 4.68, terminal olefinic C—H at 5.83 for monomer M_1, and at 6.03–6.10 for monomer M_2, suggesting that that Si—H groups in CMHS are substituted via the hydrosilylation action, and the monomers are connected to the CMHS chains. To determine the polymer compositions, the M_2 substitution degree was assessed by comparing the integrated ratio of the Ar—H signals by ^{1}H-NMR analysis in the oligomer systems. Therefore, the compositions of the oligomers and the components of the mesogens were calculated and are listed in Table I.

Thermal Analysis

The phase-transition temperatures of LC monomers M_1, M_2, and the oligomers P_1–P_7 were obtained using DSC measurement upon the second heating. The transition temperatures are summarized in Table II.

In Figure 2, M_2 undergoes a melting transition at 127°C (δH_m = 18.74 J g^{-1}) and a cholesteric–isotropic phase transition at 218°C (δH_i = 2.17 J g^{-1}) upon the second heating, and shows an isotropic–cholesteric phase transition at 187.5°C (enthalpy changes −1.01 J g^{-1}) and a crystallization transition at 86.9°C (enthalpy changes −11.95 J g^{-1}) upon cooling.

DSC thermograms of the oligomers on heating cycles are shown in Figure 3. When heated, the oligomers display two phase transition temperatures, corresponding to glass transition (T_g) and mesophase–isotropic phase transition (T_i), respectively.

It can be seen that the T_g values of the oligomers are all low, which is due to the flexible chain in the monomers and the polysiloxane backbone. Side-chain liquid crystalline polymers are most commonly composed of flexible and rigid moieties, thus the polymer backbone, sterical hinder, the rigidity of mesogenic units and the length of the flexible spacer would influence mesophase behaviors of the polymers. The results, in Table II, show that the T_g values of the oligomers increase with an increase in

Table II. Thermal Properties and LC Phase of the Oligomers

Sample	T_g(°C)	T_i(°C)	ΔT[a](°C)	T_d[b](°C)	LC phase
P_1	11.6	122.3	110.7	305.2	Ch
P_2	12.4	126.7	114.3	308.0	Ch
P_3	17.3	141.7	124.4	311.5	Ch
P_4	21.2	150.8	129.6	312.2	Ch
P_5	23.3	158.7	134.4	313.2	Ch
P_6	25.6	166.8	141.2	314.4	Ch
P_7	28.3	180.1	151.8	315.0	Ch

[a] Mesomorphic temperature range ($\Delta T = T_i - T_g$)

[b] Temperature at which the 5% weight loss occurred.

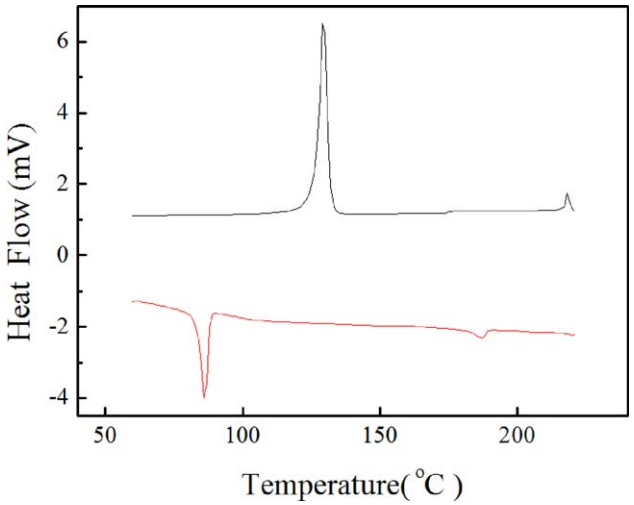

Figure 2. DSC thermograms of the monomer M_2 on the second heating and the first cooling cycles. [Color figure can be viewed in the online issue, which is available at wileyonlinelibrary.com.]

the concentration of mesogenic M_2 in the oligomers. With an increase in the concentration of M_2 units, the steric hindrance increases and flexible spacer length decreases, which making the chain flexibility decrease. As a result of a decrease in the chain flexibility, the mobility of chain segments is decreased and the T_g values are increased. At the same time, the isotropization temperature (T_i) increases for oligomers P_1–P_7. The increasing rate of T_g is slower than T_i. Consequently, the mesomorphic temperature ranges of the oligomers become broader.

The thermal stability of the oligomers was studied using TGA under a nitrogen atmosphere. Figure 4 shows TGA thermograms of some representative polymers, and the results are summarized in Table II. TGA results of the oligomers show that the decomposition temperatures (T_d) at 5% weight loss occurs greater than 300°C. The thermal stability of the oligomers reveals the bond strength of the oligomers. Because the bond energy of Si—O band is much higher than those of C—C and C—H bonds on the side chain components in the oligomer systems, the thermal stability of the oligomers would be mainly influenced by the side-chain structures of the oligomers. The synthesized oligomers contain benzene rings and long alkyl chain. The existence of the high conjugate phenyl segments and longer mesogenic side chain might cause a strong interaction between the repeating units leading to the increase of thermal stability.[3] The synthesized oligomers have a high thermal stability based on the molecular structures of the oligomers.

Texture Analysis

The optical textures of the monomers and oligomers were studied by means of POM with hot stage, and the representative optical textures are shown in Figure 5. POM results show that all monomers and oligomers exhibit an enantiotropic cholesteric phase upon heating and cooling cycles. When M_2 is heated to 148°C, the typical cholesteric oily streak texture appears [Figure 5(a)]. When the isotropic state is cooled to 152.8°C, the bright focal-conic texture appears again [Figure 5(b)]. All oligomers show similar optical textures, and P_3 is selected as an example. When P_3 is heated to 45°C, a typical cholesteric Grand-jean texture appears, as illustrated in Figure 5(c). When the sample is heated continuously, it also shows the typical cholesteric oily streak texture, as displayed in Figure 5(d). The oily streak texture is one of the most commonly observed textures of the cholesteric phase prepared between two untreated glass substrates.

X-Ray Diffraction Analysis

The cholesteric mesophase of the oligomers was also characterized by X-ray diffraction analysis. Figure 6 shows the representative XRD patterns of samples P_2, P_4, and P_7. In general, a strong and sharp peak at low angle ($1° < 2\theta < 4°$) in small angle X-ray scattering (SAXS) curves and a strong broad peak associated with lateral packing at $2\theta \approx 20°$ can be observed in wide angle X-ray diffraction (WAXD) curves for a normal smectic polymer structure. For nematic and cholesteric structures of the polymer systems, there are no strong peaks detected at low angle. But a broad peak at $2\theta \approx 20°$ or $2\theta \approx 17°$ is observed in the WAXD patterns. For all oligomers, no strong

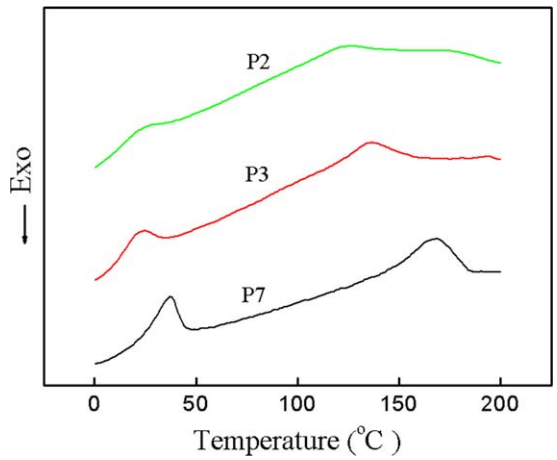

Figure 3. DSC thermograms of the oligomers on the second heating cycle. [Color figure can be viewed in the online issue, which is available at wileyonlinelibrary.com.]

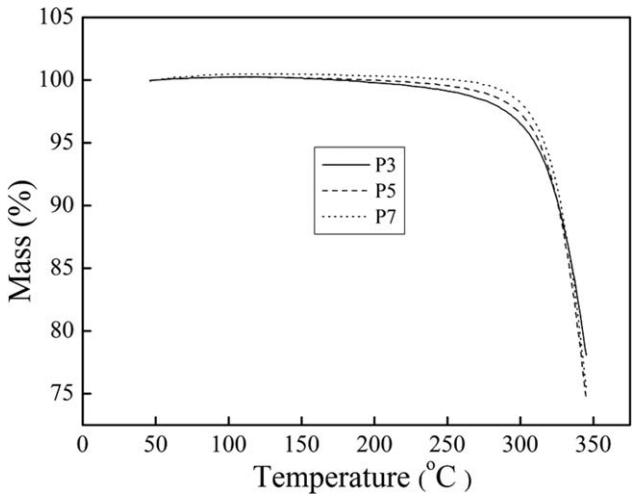

Figure 4. TGA thermographs of liquid crystal oligomers.

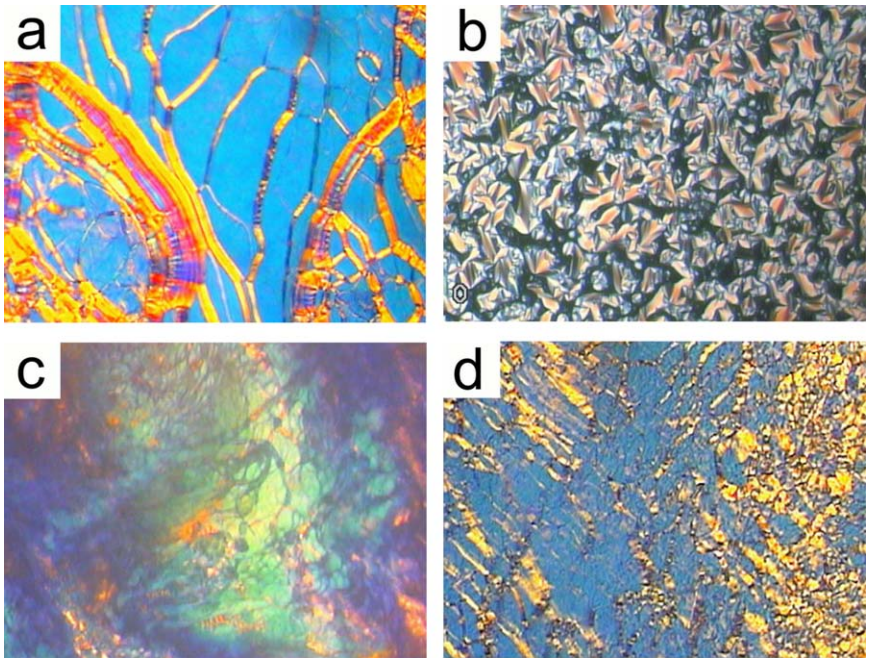

Figure 5. Some representative optical textures of the monomers and oligomers (200×): (a) Oily streak texture of M_2 upon heating to 148°C; (b) Focal-conic texture of M_2 upon cooling to 152°C; (c) Grand-jean texture of P_3 upon heating to 45°C; (d) Oily streak texture of P_3 upon heating to 77°C. [Color figure can be viewed in the online issue, which is available at wileyonlinelibrary.com.]

reflections at small angles are observed, indicating that they do not show a smectic mesophase. The XRD patterns of oligomers P_1–P_7 demonstrate that only one broad peak at 2θ of about 20° exists in the oligomers, suggesting the chiral helix structure average distance of 0.43 nm between two neighbor LC molecules within the layers of the mesophase. The intensity of the diffraction peak around $2\theta \approx 20°$ decreases with an increase in M_2 component in the oligomer systems P_1–P_7, reflecting the order between two neighbor LC molecules can be disturbed by introducing bigger size groups.

Reflection Spectra Analysis

Cholesteric mesophases exhibit interesting optical properties such as selective reflection of circular polarized light and an angular dependence of the reflected wavelength. If the reflected wavelength is in the visible range of the spectra, the cholesteric phase appears colored. The wavelength, λ_{max}, the reflected light from a cholesteric sample is given by

$$\lambda_{max} = nP\sin\phi \quad (1)$$

where n is the average refractive index of the liquid crystalline phase, P is the pitch height of the helicoidal arrangement, and φ is the incident angle of the beam. The helical pitch is an important parameter in connection with optical properties of the cholesteric phase.

The reflected wavelengths of thin films P_1–P_7 were characterized at 25.0°C without any external field, which are listed in Table I. It is shown that the maximum reflection bands shift to long wavelength from P_1 to P_7 with increasing the longer spacer component in the polymer systems, suggesting the longer spacer component induces the helical pitch P to become longer. The P of cholesteric polymers can be defined as:

$$P = \sum i(HTPixi)^{-1} \quad (2)$$

where x_i is the fraction of the chiral component, *HTP* is the helical twisting power. The *HTP* is the main parameter determining the helix pitch, which is a property of the chiral component that induces cholesteric polymers.[34] The *HTP* of a chiral component strongly depends on the molecular structure or stereochemistry of the chiral component. The shorter spacer and two benzene rings of M_2 hinder the rotation of chiral molecules around their long axes. It promotes a larger twisting of the mesogenic groups in the polymers. In contrast, the longer

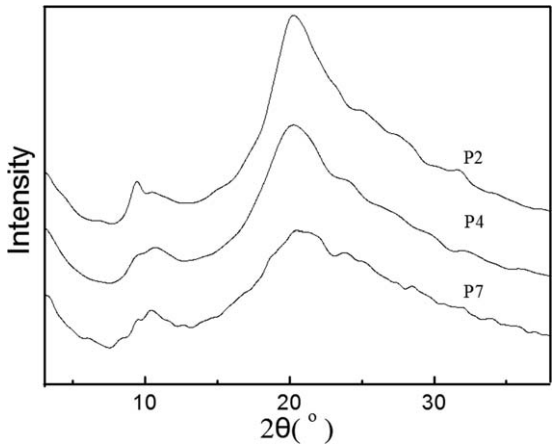

Figure 6. Representative XRD patterns of oligomers P_2, P_4, and P_7.

Applied Polymer SCIENCE

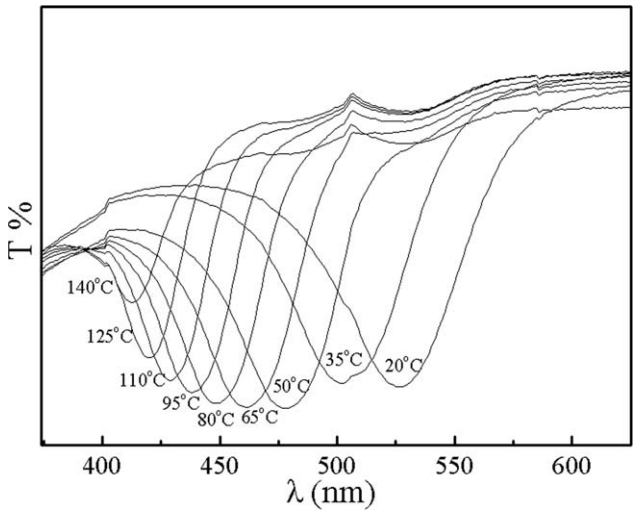

Figure 7. Selective reflection wavelength of P_4 at different temperatures.

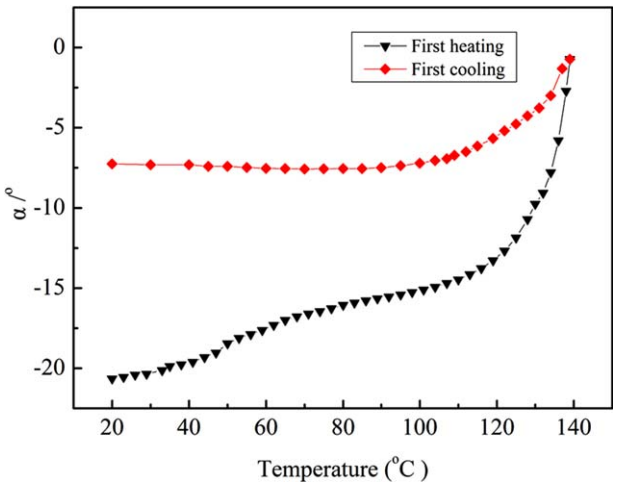

Figure 8. Optical rotation (α) of oligomer P_3 at different temperatures. [Color figure can be viewed in the online issue, which is available at wileyonlinelibrary.com.]

spacer of M_2 free rotation around the long axis of the cholesterogenic molecule will prevent a helical twist. Therefore, the *HTP* of M_1 is lower than M_2. According to eq. (2), an increase in M_1 component in the polymer systems leads to an increase in the helical pitch value of the oligomers.

Each oligomer displays different colors at room temperature, such as orange, green and blue. Figure 7 presents the temperature dependence of λ_{max} for oligomer P_3 upon the process of heating. For oligomer film P_3, with increasing the temperature in the mesomorphic state, λ_{max} markedly decreases from 533 to 405 nm, which means P_3 changes color from yellow to blue between 25°C and T_i, showing a wide range of color display (>120°C). The λ_{max} values of the oligomers are also nearly coincident during the first, second, and third heating cycles, showing that the polymer is repetitive and anti-fatigue. The biggest selective reflection wavelength (λ_{max})of polymer P_3 also changes at different reflective angle at room temperature. The λ_{max} increases from 533 to 618 nm with decreasing the reflective angles from 90° to 15°. This indicates that P_3 changes color from yellow to red with observation angles from 90° to 15° at room temperature. Therefore, it can be used as displays or linear and nonlinear optical materials.

Optical Rotation Analysis

The optical properties of chiral LC oligomers result from chiral molecules in the liquid crystalline state that induce a twist in the director of adjacent molecules thereby forming a super molecular helical structure. Compared with the monomers, the oligomers show lower specific rotation. This indicates that the concentration of optically active sites decreases because the oligomers consist of optically inactive polysiloxane. This affects the amount of optically active sites and this in turn decreases the optical rotation. In Table I, the specific rotation of oligomers P_1–P_7 decrease with an increase in monomer M_2 component in the systems. Compared with M_1, M_2 contains more benzene rings. The existence of high conjugate phenyl segments increases the molecular polarity and the molecular interactions. The higher molecular polarity and the molecular interactions hinder the rotation of chiral molecules leading to the decrease of the specific rotation.[35]

Figure 8 shows the optical rotation (α) of oligomer P_3 at different temperatures. The α value is negative at low temperature, but it becomes positive when P_3 is heated to 78°C. Furthermore, it shows the lowest and the highest α values when the sample is heated.

The relationship between the optical rotation (α) and the selective light reflection wavelength λ_{max} is given by

$$\alpha = \frac{\pi \Delta n^2 P}{4\lambda^2} \frac{1}{1-(\lambda/\lambda_{max})^2} \quad (3)$$

where Δn is the birefraction ($\Delta n = n_o - n_e$), P is the pitch height of the helicoidal arrangement, and λ is the measurement wavelength (sodium light source, $\lambda = 589$ nm).

As expressed in eq. (3), the measurement wavelength λ is fixed at the 598 nm (Na light), and the optical rotation is determined by the helical pitch and the selective reflection wavelength λ_{max}. In Figure 8, the λ_{max} of P_3 is always smaller than the measurement wavelength. According to eq. (1), the optical rotation of the oligomer is negative and the α value is decreased with increasing temperature. It also can be seen from Figure 4, the α value of film P_3 is sensitive to the applied temperature, which is decreased from $-21.7°$ to $-0.7°$ when it is heated, which is consistent with eq. ((3)). The curve of α changes smoothly on heating and cooling cycles, suggesting that LC phase is stable and the control of optical properties of the polymers is easy. The characteristics of temperature sensitivity of optical rotation and easy control of optical properties in oligomers are very helpful when they are used for polarizers.

CONCLUSIONS

A series of side-chain liquid crystalline oligomers bearing different cholesteric mesogens have been synthesized. All monomers

and oligomers show a cholesteric mesophase with very wide mesophase temperature ranges. The glass transition (T_g), mesophase–isotropic phase transition (T_i) and mesomorphic temperature range (ΔT) of the oligomers increase with an increase in M_2 component in the oligomer systems. The optical properties of the polymers were characterized by reflection spectra and optical rotation analysis. The oligomers display different colors at room temperature, showing a wide range of color display. The maximum reflection bands shift to long wavelength from P_1 to P_7 with increasing the longer spacer component in the oligomer systems, suggesting the longer spacer component induces the helical pitch P to become longer. On the other hand, the specific rotation of the oligomers smoothly decreases as temperature increasing, suggesting the specific optical rotation is sensitive to temperature and easy to modulate. It is helpful when the oligomers are used for polarizers.

ACKNOWLEDGMENTS

The authors are grateful to the National Natural Science Fundamental Committee of China and the Education Department of Yunnan Province for financial support of this study.

REFERENCES

1. Chen, B.; Deng, J. P.; Yang, W. T. *Adv. Funct. Mater.* **2011**, *21*, 2345.
2. Guo, R. W.; Li, K. X.; Cao, H. *Polymer* **2010**, *51*, 5990.
3. Liu, J. H.; Wang, Y. K.; Chen, C. C. *Polymer* **2008**, *49*, 3938.
4. Sukchol, K.; Thongyai, S.; Praserthdam, P. *J. Appl. Polym. Sci.* **2011**, *120*, 3265.
5. Meng, F. B.; Zhang, B. Y.; Lian, J. *J. Appl. Polym. Sci.* **2009**, *114*, 2195.
6. Walba, D. M.; Yang, H.; Shoemaker, R. K.; Keller, P.; Shao, R.; Coleman, D. A.; Jones, C. D.; Nakata, M.; Clark, N. A. *Chem. Mater.* **2006**, *18*, 4576.
7. Li, C. Y.; Cheng, S. Z. D.; Ge, J. J.; Bai, F.; Zhang, J. Z.; Mann, I. K.; Chien, L. C.; Harris, F. W.; Lotz, B. *J. Am. Chem. Soc.* **2000**, *122*, 72.
8. Amabilino, D. B.; Ramos, E.; Serrano, J.; Sierra, T.; Veciana, J. *J. Am. Chem. Soc.* **1998**, *120*, 9126.
9. Zhang, L. Y.; Wu, H. L.; Shen, Z. H. *J. Polym. Sci. Part A Polym. Chem.* **2011**, *49*, 3207.
10. Cui, Z. H.; Zhang, Y.; He, S. J. *Colloid Polym. Sci.* **2008**, *286*, 1553.
11. Meng, F. B.; He, X. Z.; Zhang, X. D. *Colloid Polym. Sci.* **2011**, *289*, 955.
12. Liu, J. H.; Hung, H. J.; Yang, P. *J. Polym. Sci. Part A Polym. Chem.* **2008**, *46*, 6214.
13. He, X. Z.; Zhang, B. Y.; Meng, F. B. *J. Mater. Sci.* **2010**, *45*, 201.
14. Kaspar, M.; Bubnov, A.; Sedlakova, Z. *Eur. Polym. J.* **2008**, *44*, 233.
15. Sapich, B.; Stumpe, J.; Kricheldorf, H. R. *Macromolecules* **2001**, *34*, 5694.
16. Meng, F. B.; Zhang, B. Y.; Xiao, W. Q.; Hu, T. X. *J. Appl. Polym. Sci.* **2005**, *96*, 625.
17. Mruk, R., Zentel, R. *Macromolecules* **2002**, *35*, 185.
18. Hsiue, G. H.; Chen, J. H. *Macromolecules* **1995**, *28*, 4366.
19. Hsu, L. L.; Chang, T. C.; Tsai, W. L. *J. Polym. Sci. A: Polym. Chem.* **1997**, *35*, 2843.
20. Hsiue, G. H.; Lee, R. H.; Jeng, R. J. *J. Polym. Sci. B: Polym. Phys.* **1996**, *34*, 555.
21. Hiraoka, K.; Stein, P.; Finkelmann, H. *Macromol. Chem. Phys.* **2004**, *205*, 48.
22. Shilov, S.; Gebhard, E.; Skupin, H.; Zentel, R.; Kremer, F. *Macromolecules* **1999**, *32*, 1570.
23. Brodowsky, H. M.; Boehnke, U. C.; Kremer, F. *Langmuir* **1999**, *15*, 274.
24. Kuse, Y.; Asahina, D.; Nishio. *Biomacromolecules* **2009**, *10*, 166.
25. Collings, P. Liquid Crystals-Nature's Delicate Phase of Matter; Adam Hilger: Bristol, **1990**.
26. de Gennes, P. G.; Prest, J. The Physics of Liquid Crystals; Oxford University Press: Oxford, **1993**.
27. Chiba, R.; Nishio, Y.; Sato, Y. *Biomacromolecules* **2006**, *7*, 3076.
28. Bobrovsky, A.; Boiko, N.; Shibaev, V. *Macromolecules* **2006**, *39*, 6367.
29. Schmidtke, J.; Kniesel, S.; Finkelmann, H. *Macromolecules* **2005**, *38*, 1357.
30. Shibaev, V.; Bobrovsky, A.; Boiko, N. *Prog. Polym. Sci.* **2003**, *28*, 729.
31. Singh, U., Hunte, C., Gleeson, H. *J. Appl. Polym. Sci.* **2001**, *28*, 697.
32. Hu, J. S.; Zhang, B. Y.; Pan, W.; Li, Y. H. *J. Appl. Polym. Sci.* **2006**, *99*, 2330.
33. Wang, J. W.; Meng, F. B.; Li, Y. H. *J. Appl. Polym. Sci.* **2009**, *111*, 2078.
34. Lub, J.; Nijssen, W. P. M.; Wegh, R. T. *Adv. Funct. Mater.* **2005**, *15*, 1961.
35. Hu, J. S.; Liu, C.; Zhang, X.; Meng, Q. B. *Eur. Polym. J.* **2009**, *45*, 3292.